FERMENTATIVE H$_2$ PRODUCTION FROM FOOD WASTE: PARAMETRIC ANALYSIS OF FACTOR EFFECTS

M. Akhlaghi[1], M.R. Boni[1], A. Polettini[1], R. Pomi[1], A. Rossi[1], G. De Gioannis[2,3], A. Muntoni[2,3], D. Spiga[2]

[1] Department of Civil and Environmental Engineering, University of Rome "La Sapienza", Italy

[2] Department of Civil and Environmental Engineering and Architecture, University of Cagliari, Italy

[3] IGAG – CNR (Environmental Geology and Geoengineering Institute of the National Research Council), Italy

ABSTRACT

Factorial fermentation experiments on food waste (FW) inoculated with activated sludge (AS) were conducted to investigate the effects of pH and the inoculum-to-substrate ratio (ISR [g VS$_{AS}$/g TOC$_{FW}$]) on biohydrogen production. The two parameters affected the H$_2$ yield, the fermentation rate and the biochemical pathways. The minimum and maximum yields were 41 L H$_2$/kg TOC$_{FW}$ (pH = 7.5, ISR = 1.74) and 156−160 L H$_2$/kg TOC$_{FW}$ (pH = 5.5, ISR = 0.58 and 1.74). The range of carbohydrates conversion into H$_2$ was 0.37−1.45 mol H$_2$/mol hexose, corresponding to 9.4−36.2% of the theoretical threshold. A second-order predictive model for H$_2$ production identified an optimum region at low pHs and high ISRs, with a theoretical maximum of 168 L H$_2$/kg TOC$_{FW}$ at pH = 5.5 and ISR = 1.74. The Spearman's correlation method revealed several relationships between the variables, suggesting the potentially governing metabolic pathways, which turned out to involve both hydrogenogenic pathways and competing reactions.

1

1. INTRODUCTION

Sustainable management of bio-waste is being more and more regarded as a key issue in both industrialized and emerging countries, on account of the need to reduce the potential environmental impacts from natural uncontrolled degradation and the energy exploitation perspectives that may be opened. European waste statistics indicate that ~245 Mt of municipal solid waste were generated in the EU-28 in 2016, out of which food waste (FW) is estimated to account for ~35% by weight. The environmental policies on bio-waste in most industrialized countries prescribe specific reduction targets to final disposal, promoting materials and energy recovery from bio-waste.

In this framework, biological treatment of FW is one of the key options for the environmentally sound management of biodegradable residues. More specifically, dark fermentation aimed at H_2 production ahead of further biological treatment has been widely studied for a variety of organic waste materials. In addition to the well-known positive environmental features of H_2 as an energy carrier, particularly if generated from renewable non-fossil sources, a first dark fermentation stage in AD may produce further environmental and economic advantages. Separate optimization of the acidogenic and methanogenic phases in the two-stage configuration has been reported to significantly enhance energy recovery (10–25% (Lee and Chung, 2010); 20% (De Gioannis et al., 2017); 8–43% (Schievano et al., 2014); 38% (Massanet-Nicolau et al., 2013)) compared to the conventional single-stage layout.

Various FW and kitchen waste components as well as the organic fraction of municipal solid waste (OFMSW) are recognized to be suitable and relatively inexpensive sources of biodegradable organic matter for H_2 production, mainly due to their high carbohydrate

concentration, adequate moisture content and wide availability (Alexandropoulou et al., 2018; Alibardi and Cossu, 2016, 2015; Dong et al., 2009; Kim et al., 2011b, 2004; Kobayashi et al., 2012; Liu et al., 2006; Nazlina et al., 2011; Tawfik and El-Qelish, 2012; Wang and Zhao, 2009; Zhu et al., 2008).

Fermentative H_2 production depends on several factors, acting either synergistically or antagonistically. Factors include substrate-related characteristics (substrate composition, concentration and pre-treatment methods), microorganisms-related characteristics (inoculum type [pure/mixed cultures], inoculum pre-treatment and selection methods, inoculum-to-substrate ratio [ISR]), and control and operating parameters (temperature, pH, organic loading rate, hydraulic and cell residence time, reactor type and operation regime) (Alexandropoulou et al., 2018; Alibardi and Cossu, 2016; Ghimire et al., 2016; Tawfik and El-Qelish, 2014; Van Ginkel et al., 2001). Therefore, prediction and optimization of the fermentation pathways requires both the individual effects of the relevant parameters and their mutual interactions to be described and quantified accurately. To this aim, since investigations based on a "one variable at a time" approach are considered to be inadequate to provide a reliable understanding of the process (Akhlaghi et al., 2017), alternative experimental design and data analysis methods should be adopted to pick the complex interrelations among the relevant factors.

Under batch conditions and for a given substrate type, the fermentation process is chiefly governed by the operating pH and the availability of microorganisms. In particular, the operating pH is recognized to govern the substrate hydrolysis yield, the activity of hydrogenase, the energy utilization yield by the biomass as well as the metabolic pathways (Kim et al., 2011a; Rodríguez et al., 2006). The availability of microorganisms in the system is measured through either the ISR or its reciprocal, the food-to-microorganisms (F/M) ratio. The relative amounts of substrate and biomass in the system can determine a variety of conditions ranging from substrate-limited to substrate-sufficient growth (Liu, 1996), in turn affecting the yield of substrate conversion into

the metabolic products (Cappai et al., 2015). For a more detailed review of the individual effects of pH and ISR on the fermentation process, the reader is referred to previous literature studies (see e.g. (Akhlaghi et al., 2017; Cappai et al., 2018, 2014, De Gioannis et al., 2014, 2013, 2009; Ghimire et al., 2015) and references therein). Although the individual effects of pH and ISR on the kinetics and yield of fermentative H_2 production from organic residues have been widely investigated, so far relatively few studies (Ghimire et al., 2016; Pan et al., 2008; Van Ginkel et al., 2001) have been conducted on their combined influence, particularly for food waste. It is also emphasized that most studies have focused on the influence of the initial pH only, while that of the operating pH (which, on the other hand, is by far more relevant for the biochemical reactions) has been largely overlooked. The present work attempts to fill in the gaps on the joint effects of pH and ISR on hydrogenogenic fermentation of organic waste by means of a dedicate experimental campaign on a food waste sample that was deemed to be representative of the typical composition of the food fraction of Italian municipal solid waste (Andreasi Bassi et al., 2017). The main novel contribution to the knowledge in the field lies in the identification of the relationships and mutual interactions among the operating pH, ISR and the response variables of the fermentation process of the food waste of concern. To this aim, a systematic approach based on factorial experiments was adopted, followed by the identification of hidden relationships among the factors and the response variables by means of statistical analysis tools and empirical modelling of parameters effects. All such tools were combined to interpret the complex biochemical transformations involved in the process, identify the optimal conditions for hydrogenogenesis and provide indications for further enhancing the process yield.

2. MATERIALS AND METHODS

2.1 Feedstock and inoculum

4

The substrate used in this study was source-separated OFMSW coming from door-to-door collection of municipal waste in a medium-size city located in central Italy. The OFMSW was manually sorted to select food components and then homogenised to ensure the reproducibility of sub-samples used for the characterization and fermentation tests. The obtained waste was deemed to be representative of the typical composition of the food fraction of Italian municipal solid waste (Andreasi Bassi et al., 2017).

The total solids (TS) content of the homogenised samples was adjusted through the addition of tap water to a final TS content of 4.3% by weight. The samples were kept frozen until use. Activated sludge (AS) from the aerobic unit of a municipal wastewater treatment plant was used as the inoculum. AS was considered a suitable biomass source due to the presence of facultative bacteria, which typically have a high growth rate and the ability to rapidly recover from accidental oxygen intrusion. The AS samples were kept frozen until use. Before fermentation, the AS was unfrozen and heat-shocked (105 °C, 30 min) prior to mixing with FW, in order to inactivate methanogens and harvest hydrogen producers. These are known to be capable of producing endospores when subjected to harsh conditions; the endospores can then germinate back to their active vegetative state when suitable growth conditions are established (Fan et al., 2004; Kim et al., 2011a). The heat-shock treatment (HST) conditions were selected on the basis of previous investigations (Cappai et al., 2014; De Gioannis et al., 2014).

The characterization parameters for the FW and AS samples are reported in Table 1.

2.2 Experimental set-up

Batch fermentation tests were conducted in mechanically stirred glass reactors connected to an automatic system for data recording and continuous pH control by means of NaOH addition. The reactors (total volume = 1 L, working volume = 0.5 L) were maintained under mesophilic conditions (T = 39±1 °C). Eudiometers were used to measure the biogas volume produced in

each reactor adopting the volume displacement principle; to this aim, each eudiometer was filled with a NaCl-saturated solution acidified with H_2SO_4 to pH = 2 to prevent gas dissolution. Automatic recording of the biogas volume was accomplished through an electronic load cell that weighed the volume of solution displaced from the eudiometers into a storage tank. Corrections for liquid and gas densities were made to convert the measured liquid weight to the corresponding biogas volume. The latter was then further converted to standard temperature and pressure conditions (T = 273.15 K, P = 10^5 Pa).

Before the onset of the experiments, the reactors were flushed with N_2 gas for a few minutes to drive off air from the reactor headspace.

Nine batch fermentation runs (see Table 2) were arranged according to a full factorial design in two factors (pH and ISR) at three levels: pH = 5.5, 6.5, 7.5, ISR = 1.74, 0.58, 0.19 g VS_{AS}/g TOC_{FW} (corresponding to FW/AS ratios of 25:75, 50:50, 75:25). The use of factorial designs at two (with possible addition of optional centre points) or three levels is common practice in the statistical design of experiments. Each fermentation run was performed in triplicate and the results will be reported in the following as the average of replicate data. Each test was stopped once any appreciable biogas production could be no longer detected.

2.3 Analytical methods

A 10-mL volume of digestate was periodically sampled from the reactors during the experiments. The sampling frequency was based on the observed biogas production profile over time. An aliquot of the samples to be analysed for soluble parameters was also filtered onto a 1.2 μm membrane.

The process performance was evaluated by monitoring the volumetric amount and composition of the biogas produced, as well as the concentration of total solids (TS), volatile solids (VS), total organic carbon (TOC), dissolved organic carbon (DOC), soluble carbohydrates, volatile

6

fatty acids (VFAs) and ethanol.

The biogas was sampled from the eudiometers with a gastight syringe and analysed through a gas chromatograph (Model 3600 CX, VARIAN) equipped with a thermal conductivity detector and 2-m stainless-steel packed column (ShinCarbon ST) with an inner diameter of 1 mm. The operation temperatures of injector and detector were 100 and 130 °C, respectively, with He as the carrier gas. The oven temperature was initially set at 80 °C and subsequently increased to 100 °C at 2 °C/min.

The VFAs (acetic [HAc], propionic [HPr], butyric + iso-butyric [HBu], valeric + isovaleric [HVal], hexanoic + isohexanoic [HHex], heptanoic [HHep]) concentration in the digestate was determined in 0.2-µm filtered and HCl-acidified (pH = 2) liquid effluent with a gas chromatograph equipped with a flame ionization detector (FID) and a 30 m capillary column (TRB-WAX) with an inner diameter of 0.53 mm. The temperatures of the detector and the injector were 270 and 250 °C, respectively. The oven temperature was initially set at 60 °C, held for 3 min at this value, subsequently increased to 180 °C at a rate of 10 °C/min and finally increased to 220 °C at a rate of 30 °C/min and held for 2 min. All the analytical determinations were performed in duplicate.

To describe the time evolution of H_2 production, the commonly adopted Gompertz bacterial growth model was modified to improve fitting for the two-staged biogas production already observed in our previous investigations (Akhlaghi et al., 2017; De Gioannis et al., 2014) and also confirmed in the present study. The two-stage modified Gompertz equation used in the present work has the form:

$$HPY(t) = HPY_{max,1} \exp\left\{- \exp\left[\frac{R_{m1} \cdot e}{HPY_{max,1}}(\lambda_1 - t) + 1\right]\right\} + HPY_{max,2} \exp\left\{- \exp\left[\frac{R_{m2} \cdot e}{HPY_{max,2}}(\lambda_2 - t) + 1\right]\right\} \quad (1)$$

where:

HPY = cumulative H_2 production yield at time t

$HPY_{max,1}$, $HPY_{max,2}$ = maximum theoretical H_2 production yield for each stage

R_{m1}, R_{m2} = maximum H_2 production rate of each stage

λ_1, λ_2 = lag phase duration of each stage

The existence of fermentation stages described by different kinetic parameters is possibly associated to the presence of different substrate components that are degraded at different rates during the process.

Fitting of the experimental data with Equation (1) was accomplished by means of least-square non-linear regression using Table Curve2D®. In order to evaluate the overall duration of the process, the time (t_{95}-H_2) required for H_2 production to attain 95% of the maximum yield was also calculated.

2.4 Statistical analyses

As a first screening, in order to single out monotonic correlations between the variables of interest the Spearman's rank-order correlation coefficients were calculated. Such coefficients provide a measure of the strength and direction of association between pairs of variables, where values of +1 and −1 mean, respectively, a perfect positive or negative correlation between the variables, while a value of 0 implies no correlation. Spearman's correlation coefficients measure not only linear, but all kinds of monotonic correlations. The investigated variables included both the operating parameters and the main response variables of the process. The Spearman's coefficients for each pair of variables were graphically visualized in a correlation matrix by means of the *corrplot* package (Wei and Simko, 2016) developed for application with the R software (R Development Core Team, 2009).

Further analyses were aimed at identifying statistically significant effects and interactions of pH and ISR on the process performance. The statistical t-test was adopted at a confidence level of

8

95%. The response surfaces for the process were derived through the second-order polynomial model given in Equation (2), which expresses each response variable, y, as a function of the main (linear and quadratic) and interaction (linear × linear) effects of the two factors:

$$y = \beta_0 + \beta_1 x_1 + \beta_2 x_2 + \beta_{11} x_1^2 + \beta_{22} x_2^2 + \beta_{12} x_1 x_2 + \varepsilon \qquad (2)$$

where:

x_1, x_2 = levels of the two factors

ε = random error component

β_0 = zero-order coefficient

β_1, β_2 = linear component coefficients

β_{11}, β_{22}, β_{12} = quadratic component coefficients

The estimation of the coefficients of the polynomial model was made through least-square regression of the experimental data using the *rsm* package (Lenth, 2009) implemented in R.

3. RESULTS AND DISCUSSION

3.1 H$_2$ production yield

The specific hydrogen production yield (SHPY) per unit of initial TOC of FW in the mixture is reported in Figure 1. Individual data points are direct H$_2$ production measurements, while continuous lines represent the two-stage Gompertz production curves derived from model (1). The results of fitting of H$_2$ production data with model (1) are reported in Table 3 in terms of parameter values and related statistics. It is worth mentioning that the degree of data fitting by the two-stage Gompertz model turned out to be in all cases higher than for the conventional Gompertz equation (results not shown).

The fermentation tests yielded in all cases (with the exception of run 25FW pH7.5) a relevant H$_2$ production, in excess of 75 L H$_2$/kg TOC$_{FW}$. The biogas produced was always found to be

composed of H_2 and CO_2 only, again with the exception of run 25FW pH7.5, in which CH_4 contents of 10–24% vol. were also detected. In all the other tests, the measured volumetric H_2 concentrations in the biogas were 47–69% at pH 5.5, 57–75% at pH 6.5 and 85–94% at pH 7.5. As already pointed out in our previous studies (Akhlaghi et al., 2017; Cappai et al., 2014; De Gioannis et al., 2014), the observed trend of the volumetric H_2 content as a function of pH was to be related to the higher CO_2 solubility in water at higher pH conditions rather than to a direct effect of these on the fermentation reactions.

The fermentation process was strongly affected by pH and ISR, and different combinations of the two factors resulted in large changes in both the final yield and time evolution. The correlation matrix showing the Spearman's rank correlation coefficients for all the variables of interest is reported in Figure 2. Each cell of the correlation matrix reports a circle whose size and colour shade show graphically the value of the Spearman's correlation coefficient (blue shades: positive correlation; red shades: negative correlation).

The lowest SHPY (as derived from the two-stage Gompertz model), equal to 41.5 L H_2/kg TOC_{FW}, was associated to FW = 25% (ISR = 1.74 g VS_{AS}/g TOC_{FW}) and pH = 7.5. The maximum SHPY (160.3 L H_2/kg TOC_{FW}) was attained at FW = 25% (ISR = 1.74 g VS_{AS}/g TOC_{FW}) and pH = 5.5. The test conducted at FW = 50% (ISR = 0.58 g VS_{AS}/g TOC_{FW}) and pH = 5.5 displayed a SHPY of 156.4 L H_2/kg TOC_{FW}, that was still close to the maximum value attained. The existence of a negative linear correlation between SHPY and pH is clear from data in Figure 2, confirming that the optimum region for H_2 production corresponded to slightly acidic pHs. On the other hand, while no simple linear correlation turned out to hold between SHPY and ISR (see Figure 2), subsequent statistical analyses indicated a more complex, higher-order relationship between the two (see below for details).

The region of maximum H_2 production corresponds to the same combination of pH and ISR identified in a companion study where cheese whey (CW) was used as the substrate for the

10

fermentation experiments (Akhlaghi et al., 2017). It should also be emphasized that our previous study on fermentation of synthetic food waste (Cappai et al., 2014) located the optimum region at pH = 6.5 and ISR = 0.14 g VS_{AS}/g TOC_{FW}, which is somewhat different from the condition identified in the present work. On one instance, it may well be that the real food waste sample used in this study had a different content of the relevant components for hydrogenogenesis compared to the synthetic food waste, which may have resulted in different effects of the operating parameters on the process performance. Yet, it should also be taken into account that a wider range of ISR values and a larger number of combinations between the two factors was investigated in the present work, reasonably leading to a more accurate identification of the optimal fermentation conditions.

The optimal SHPY measured here falls within the upper range of values documented by previous literature studies on batch fermentation of real food waste, which are summarized in the Supplementary Information document.

3.2 H_2 production kinetics

Most tests displayed a two-staged biogas production, which was generally more pronounced at higher ISR values. Multi-staged degradation is likely related to different substrate constituents being consumed at different rates. Similar conclusions were obtained in a fermentation study on different sugars (Rosales-Colunga et al., 2012), in which the rates of H_2 and metabolic products generation were found to be affected by the type of sugar substrate used.

An additional distinguishing feature of the fermentation experiments was the decrease in the biogas volume towards the end of the test, particularly at pH = 7.5. As discussed below, this was likely associated to H_2-consuming pathways that presumably became prevalent upon depletion of the preferred substrate for hydrogenogenesis.

The kinetics of the fermentation process was investigated through the parameter t_{95}-H_2 defined in

11

Section 2.3, adopted as an estimate of the total process duration. The other kinetic parameters of the modified Gompertz equation, R_m and λ, could not be adopted to comparatively evaluate the process kinetics under the different experimental conditions, since they are in turn dependent on the maximum yield attained and affected by the existence of sequential substrate degradation phases. As noted for SHPY, t_{95}-H_2 was also found to largely depend on both pH and ISR (see Figure 2 and Figure 1 d). At a given ISR, t_{95}-H_2 appeared to be negatively correlated with pH, while the trend with ISR was non-monotonic (see below for further considerations). The observed ranges for t_{95}-H_2 were 18−65 h at pH 5.5, 11−20 h at pH 6.5 and 5−16 h at pH 7.5. It should be mentioned that one of the replicates for the 75FW pH5.5 run displayed an unreasonably large value for t_{95}-H_2, which was therefore dropped from the dataset in view of the statistical analyses; the corrected average value for t_{95}-H_2 after removing the outlier was found to be 42.8 h. It was also evident that the best performance in terms of H_2 production was not mirrored by a faster fermentation kinetics, which clearly points at antagonistic reactions playing a role during the process itself.

3.3 Response surfaces for H_2 production

The response surfaces for SHPY and t_{95}-H_2 were derived by fitting the experimental data with the quadratic model (2), the results of which are depicted in Figure 3 (a) and (b) as contour plots versus pH and ISR. The curvature of the response surfaces indicates the importance of the second- order terms (quadratic effects of the factors and their interactions) to reliably predict H_2 production, as already observed in our previous study on CW fermentation (Akhlaghi et al., 2017). The second-order model provided a good description of the experimental results for SHPY, and the correlation between the measured and the predicted data showed an R^2 of 0.87. The shape of the contour plots also suggests that pH had a more relevant effect on SHPY than on t_{95}-H_2, particularly in the upper ISR region ($> \sim 0.6$ g VS/g TOC). The optimum region for H_2

production within the explored range of values was found to be located at the upper left of the plots in Figure 3 a), with a theoretical maximum of 168 L H_2/kg TOC_{FW} at pH = 5.5 and ISR = 1.74 g VS_{AS}/g TOC_{FW}.

The results of the second-order model adopted to describe the effects of the two factors show that some remarkable H_2 production yields can be attained provided that pH and ISR are selected within appropriate ranges. SHPY in excess of 120 L H_2/kg TOC_{FW} can be achieved under a variety of combinations for pHs $\leq$ 7.0 and ISRs $\geq$ 0.32 g VS_{AS}/g TOC_{FW}; increasing the target for SHPY to 150 L H_2/kg TOC_{FW} requires a narrower range of values, with pH $\leq$ 6.2 and ISR $\geq$ 0.81 g VS_{AS}/g TOC_{FW}.

As mentioned, the overall duration of the process (see Figure 3 b)) was affected by ISR more than by pH. The influence of pH was only evident in the central region for ISR (ISR = 0.8–1.2 g VS_{AS}/g TOC_{FW}), where the predicted range for t_{95}-H_2 was 0–15 h.

3.4 Organic matter degradation

Figure 4 compares TOC and soluble carbohydrates in terms of time evolution of concentrations normalized by the corresponding initial value. The overall TOC degradation was very low for all tests and roughly linear over time, ranging from 2% for the 50FW pH7.5 run to 19% for the 25FW pH5.5 run. This clearly indicates that only a minor fraction of the substrate organic matter is mineralized during the process, the major portion being rather retained in the system in the form of either metabolic products, non-degraded carbon or microbial cells.

Unlike TOC, soluble carbohydrates displayed some significant degradation during the process, with a distinguishing shape of the concentration-vs.-time curves. As observed in our previous studies on both CW and FW (Akhlaghi et al., 2017; Cappai et al., 2014; De Gioannis et al., 2014), soluble carbohydrates were rapidly consumed during the fermentation process. This confirms the widely demonstrated carbohydrate characteristic of being the preferred substrate for

H$_2$ production (Alibardi and Cossu, 2016, 2015; Chatellard et al., 2016; De Gioannis et al., 2014, 2013; Nazlina et al., 2011; Rosales-Colunga et al., 2012; Santos et al., 2012). Soluble carbohydrate removal always exceeded 90% and in most cases lay in the range 94−96%, indicating that the degradation process was almost complete for such species. Apart from the runs 25FW pH7.5 and 50FW pH7.5 (for which the few digestate samples analysed did not allow to derive considerations about the carbohydrate utilization rate), all the remaining data were found to follow a first-order decay law, confirming the findings of our previous studies on CW (Akhlaghi et al., 2017; De Gioannis et al., 2014). The time required to attain 95% carbohydrate removal, t_{95}-carb, was derived from the first-order interpolating curves describing the time evolution of carbohydrates. The calculated values ranged from a minimum of 12 h for the 25FW pH6.5 run to a maximum of 81 h for the 75FW pH5.5 run. As mentioned above, no such calculations could be done for the 25FW pH7.5 and 50FW pH7.5 tests. All the other experiments displayed t_{95}-carb values below 34 h, indicating a relatively high carbohydrate consumption rate during the fermentation process. The positive linear correlation observed between t_{95}-carb and t_{95}-H$_2$ (see Figure 2) again clearly demonstrates that the hydrogenogenic process is closely governed by carbohydrate utilization.

3.5 Metabolites production and analysis of the metabolic pathways

Since, unlike carbohydrate degradation, SHPY varied among the tests, the metabolic pathways governing the fermentation process were likely affected by the specific experimental conditions adopted. In order to identify the prevailing biochemical reactions, the analysis of the relevant metabolic products was conducted. The metabolites concentrations over time are reported in Figure 5 along with the corresponding H$_2$ production. Valerate and heptanoate were always lower than the analytical detection limit (10 ppm), while hexanoate was detected, although at notably low concentrations, for a limited number of digestate samples only. Acetate and butyrate

14

were, along with ethanol, the main metabolic products measured in the digestate; propionate was also found in the samples, although it was detected at relevant concentrations towards the final fermentation stages only. The correlation analysis of the variables showed that the specific concentrations (mmol/kg TOC_{FW}) of acetate, butyrate and propionate all positively correlated with ISR (see Figure 2), suggesting that increased amounts of biomass in the system promoted substrate conversion into the metabolic products. The production of multiple metabolic products from FW has widely been reported (see e.g. (Alexandropoulou et al., 2018; Cappai et al., 2014; Cheng et al., 2016; Han et al., 2016; Kim et al., 2011b; Reddy et al., 2018)). According to our considerations (see below), this clearly points out at reaction pathways with different H_2 generation yields and likely being mutually competitive as well. However, a univocal identification of the individual pathways proves rather troublesome, given the complexity of the microbial reactions involved during fermentation, particularly due to the wide variety of the substrate and inoculum constituents. However, the results of digestate characterization in terms of concentrations of metabolites and their relative ratios can still provide interesting indications about the prevailing biochemical mechanisms. In particular, among the analysed metabolic products, acetate displayed the highest concentrations along the test. The final content lay in the ranges (in mol HAc/kg TOC_{FW}) 2.2–3.5 at pH 5.5, 4.3–9.6 at pH 6.5, and 6.2–13.7 at pH 7.5. Ethanol was prevalent over butyrate at the initial stages of the process, while the relative concentration of the two species tended gradually to reverse as time elapsed. Another distinguishing feature, already observed in our previous experiments on CW (Akhlaghi et al., 2017), was related to the progressively increasing trend of the HBu/HAc molar ratio over time and the positive correlation it displayed with SHPY (or negative correlation with pH; see Figure 2). SHPY was also found to correlate with the butyrate molar fraction of the total metabolites analysed (see Figure 2), indicating larger proportions of butyrate in the digestate being associated to higher H_2 yields. While in principle the yield of the commonly acknowledged H_2-

15

producing pathways (see reactions (3) and (4) below) would not support this finding, the positive

correlation between butyrate and H_2 production has been previously reported by several studies

(see e.g. (Ghimire et al., 2018; Guo et al., 2014; Kim et al., 2006; Noblecourt et al., 2018)) and is

motivated by the fact that butyrate is the only species univocally associated to H_2 generation. To

this regard, the absence of a direct monotonic correlation between acetate and SHPY may

support this statement, likely resulting from the masking effect of competing processes, as

detailed in the following discussion. Some authors (Michel-Savin et al., 1990) also observed a

higher acetate production by *Clostridium tyrobutyricum* during the initial fermentation stages

corresponding to the exponential growth phase of the biomass, which may be justified by the

higher ATP generation from acetate than from butyrate production, with a more efficient energy

supply to the microbial cells. In the same study, butyrate was on the other hand found to form at

lower biomass growth rates, which possibly explains the increasing trend of the HBu/HAc ratio

with time observed in our experiments.

The concomitant presence of different metabolic products was taken as an evidence of the

existence of multiple biochemical pathways during the experiments. Indeed, the clostridial-type

fermentation of hexose-type carbohydrates would yield 2 moles of H_2 per mole of either acetate

or butyrate produced, as indicated by reactions (3) and (4) (see e.g. (Ljungdahl et al., 1989)):

$$C_6H_{12}O_6 + 2H_2O \rightarrow 4H_2 + 2CO_2 + 2CH_3COOH \tag{3}$$

$$C_6H_{12}O_6 \rightarrow 2H_2 + 2CO_2 + CH_3CH_2CH_2COOH \tag{4}$$

Propionic fermentation represents a competitive pathway for hydrogenogenesis, since the

corresponding reaction (Eq. (5) (Antonopoulou et al., 2008)) consumes 1 mol of H_2 per mol of

propionate produced:

$$C_6H_{12}O_6 + 2H_2 \rightarrow 2CH_3CH_2COOH + 2H_2O \tag{5}$$

The presence of both acetate and butyrate in the digestate suggests that reactions (3) and (4)

would occur concomitantly during the tests. The facts that SHPY was positively correlated with

the HBu/HAc molar ratio and that this ratio increased over time may either indicate a higher rate

for reaction (4) compared to (3) (likely to consume the excess reducing equivalent produced

during the process (Ljungdahl et al., 1989)), or acetate production deriving from additional

pathways, which possibly overlapped and competed with the hydrogenogenic reactions. The

latter was proposed by other authors (Ghimire et al., 2018) as a tentative explanation of the

nature and relative amount of the metabolic products observed. Potential candidates for

competing reactions may include: a) heterotrophic/autotrophic homoacetogenesis (Eqs. (6) and

(7) (Ljungdahl et al., 1989; Saady, 2013), the latter even involving H_2 consumption); b) lactate

plus acetate production by homofermentative lactic acid bacteria (Eq. (8) (Antonopoulou et al.,

2008)), or 3) propionate plus acetate production from lactate (Eq. (9) (Ljungdahl et al., 1989)).

The high positive correlation between the acetate and propionate concentrations evidenced by

the Spearman's coefficient in Figure 2 suggests that, among the competing pathways, reaction

(9) may have played a role during the process, as already proposed by (Guo et al., 2014).

$$C_6H_{12}O_6 \rightarrow 3CH_3COOH \tag{6}$$

$$2CO_2 + 4\,H_2 \rightarrow CH_3COOH + 2H_2O \tag{7}$$

$$2C_6H_{12}O_6 \rightarrow 3CH_3COOH + 2CH_3CHOHCOOH \tag{8}$$

$$3CH_3CHOHCOOH \rightarrow 2CH_3CH_2COOH + CH_3COOH + CO_2 + H_2O \tag{9}$$

The ratio between the total amount of metabolic products analysed and DOC at the end of the

tests was rather different throughout the experimental runs, with values of 47−63% at pH 5.5,

23−35% at pH 6.5, and 33−82% at pH 7.5. This suggests that either non-degraded dissolved

carbon or other metabolic products in addition to the analysed species were present in the

digestion system, also possibly indicating a more complex set of metabolic reactions than that

expressed by Equations (3)−(9). The specific contribution of the individual metabolic pathways

taking place during the process is rather hard to quantify, even more so considering the variety of

the potential metabolic products formed. Taking into account the main processes commonly

17

related to H_2 production (mainly reactions (3), (4) and (5)), the measured production of acetate, butyrate and propionate was used to stoichiometrically calculate a theoretical SHPY ($SHPY_{theor}$) as illustrated in previous papers (Akhlaghi et al., 2017; Cappai et al., 2014; De Gioannis et al., 2014). The ratio between the observed and theoretical SHPY (see Figure 6 a)) displayed relatively high values at pHs 5.5 and 6.5 (with ranges of 67−88% and 79−88%, respectively), indicating a comparatively small contribution of alternative metabolic pathways to H_2 production. At pH 7.5 the $SHPY_{obs}$ was only 6−60% of $SHPY_{theor}$, which clearly suggests that a significant portion of the measured metabolic products derived from other pathways than those expressed by reactions (3)−(5). Interestingly, the $SHPY_{obs}/SHPY_{theor}$ ratio correlated negatively with the fraction of DOC retrieved in the measured metabolic products ($\Sigma(C_{metab.\ prod.})$/DOC; see Figure 2 and Figure 6 a)). This may be interpreted considering that a closer agreement between $SHPY_{obs}$ and $SHPY_{theor}$ was generally associated to metabolic pathways producing a different pool of products (not interfering with H_2 production) in addition to those resulting from reactions (3)−(5). Conversely, low $SHPY_{obs}/SHPY_{theor}$ ratios (particularly at pH 7.5) were most likely the result of competing reactions involving metabolic products in common with clostridial fermentation, which reduced $SHPY_{obs}$ compared to the anticipated theoretical value. In such cases, this in turn also indicates that a non-negligible portion of the substrate degraded did not take part in hydrogenogenic reactions.

The calculated conversion yield of carbohydrates into H_2 was found to lie in the range 0.37 − 1.45 mol H_2/mol hexose, corresponding (on account of the so-called Thauer limit of 4 mol H_2/mol hexose) to 9.4−36.2% of the theoretical conversion attainable. These values are comparable to those achieved in our previous experiments on both FW and CW (Akhlaghi et al., 2017; Cappai et al., 2014; De Gioannis et al., 2013) and within the range reported in the literature.

3.6 Carbon mass balance

The carbon mass balance at the end of the experiments was calculated to further infer on the substrate degradation mechanisms. The following contributions to total C were accounted for (see Figure 6 b)): 1) C in the form of the analysed metabolic products (VFAs and ethanol); 2) residual organic C, in both soluble and particulate forms (C present as non-degraded organic compounds and/or other metabolic products not accounted for in item 1), as well as microbial cells); 3) dissolved inorganic C; 4) C removed through periodic digestate sampling; 5) gasified C. The term "balance" in Figure 6 b) represents the C mass that was apparently lost due to either inaccuracies in the analytical measurements or sample inhomogeneity and was thus required to close the materials balance. All contributions to the mass balance were calculated from direct measurements in the liquid and gaseous phases, with the exception of dissolved inorganic C, that was indirectly estimated through chemical equilibrium considerations based on CO_2 solubility as a function of pH and temperature. The program was run with the operating pH, the digestate temperature and the measured CO_2 pressure as the input values and yielded the total inorganic C concentration in the liquid phase at thermodynamic equilibrium as the output.

While the initial partitioning of DOC was observed to have changed considerably at the end of the runs (the $\Sigma(C_{metab.\ prod.})$/DOC ratio increasing from 7.2–12.5% to 55.3–96.2%), yet the highest share (81–98%) of the initial TOC turned out to be retained in the digestate as residual C (34–66% as soluble species [with 14–28% ascribed to the measured metabolites] and 24–47% in particulate forms). The amount of gasified C was always found to account for a low fraction (3.5–7.4%) of the initial TOC.

4. CONCLUSIONS

- pH and ISR exerted individual and synergistic effects on the H_2 yield, the fermentation kinetics and the biochemical pathways. This implies that careful optimization of the

19

operating conditions is required to maximize H_2 production

- the hydrogenogenic process was strongly related to carbohydrate degradation. This provides useful indications on the types of organic residues potentially suitable for H_2 production

- the second-order predictive model was used to identify the theoretical optimal region for H_2 production (168 L H_2/kg TOC_{FW}), which may then be subjected to further refinement experiments to account for higher-order effects of the factors

- the governing metabolic pathways were found to involve both hydrogenogenic and competing reactions. Enhancing organic matter conversion into H_2 beyond the maximum observed in the present study (1.45 mol H_2/mol hexose) would thus require inhibition of H_2-scavenging pathways

- changes in waste composition due to geographical or seasonal factors, with particular reference to the carbohydrate content, are expected to imply different H_2 yields, thus requiring specific investigation of the fermentation process

SUPPLEMENTARY INFORMATION

E-supplementary data for this work can be found in the e-version of this manuscript online.

REFERENCES

Akhlaghi, M., Boni, M.R., De Gioannis, G., Muntoni, A., Polettini, A., Pomi, R., Rossi, A., Spiga, D., 2017. A parametric response surface study of fermentative hydrogen production from cheese whey. Bioresour. Technol. 244, 473–483. doi:10.1016/j.biortech.2017.07.158

Alexandropoulou, M., Antonopoulou, G., Trably, E., Carrere, H., Lyberatos, G., 2018. Continuous biohydrogen production from a food industry waste: Influence of operational parameters and microbial community analysis. J. Clean. Prod. 174, 1054–1063.

doi:10.1016/J.JCLEPRO.2017.11.078

Alibardi, L., Cossu, R., 2016. Effects of carbohydrate, protein and lipid content of organic waste on hydrogen production and fermentation products. Waste Manag. 47, 69–77. doi:10.1016/j.wasman.2015.07.049

Alibardi, L., Cossu, R., 2015. Composition variability of the organic fraction of municipal solid waste and effects on hydrogen and methane production potentials. Waste Manag. 36, 147–55. doi:10.1016/j.wasman.2014.11.019

Andreasi Bassi, S., Christensen, T.H., Damgaard, A., 2017. Environmental performance of household waste management in Europe - An example of 7 countries. Waste Manag. 69, 545–557. doi:10.1016/J.WASMAN.2017.07.042

Antonopoulou, G., Gavala, H.N., Skiadas, I. V, Angelopoulos, K., Lyberatos, G., 2008. Biofuels generation from sweet sorghum: fermentative hydrogen production and anaerobic digestion of the remaining biomass. Bioresour. Technol. 99, 110–9. doi:10.1016/j.biortech.2006.11.048

Cappai, G., De Gioannis, G., Friargiu, M., Massi, E., Muntoni, A., Polettini, A., Pomi, R., Spiga, D., 2014. An experimental study on fermentative H2 production from food waste as affected by pH. Waste Manag. 34. doi:10.1016/j.wasman.2014.04.014

Cappai, G., De Gioannis, G., Muntoni, A., Polettini, A., Pomi, R., Rossi, A., Spiga, D., 2018. Influence of the inoculum to substrate ratio on fermentative hydrogen production from food waste. Int. J. Hydrogen Energy (submitted).

Cappai, G., De Gioannis, G., Muntoni, A., Polettini, A., Pomi, R., Spiga, D., 2015. Effect of inoculum to substrate ratio (ISR) on hydrogen production through dark fermentation of food waste, in: Cossu, R., He, P.., Kjeldsen, P., Matsufuji, Y., Reinhart, D., Stegmann, R. (Eds.), Sardinia 2015, Fifteenth International Waste Management and Landfill Symposium, S. Margherita Di Pula, Cagliari, Italy, 5-9 October 2015.

21

Chatellard, L., Trably, E., Carrère, H., 2016. The type of carbohydrates specifically selects microbial community structures and fermentation patterns. Bioresour. Technol. 221, 541–549. doi:10.1016/J.BIORTECH.2016.09.084

Cheng, J., Ding, L., Lin, R., Yue, L., Liu, J., Zhou, J., Cen, K., 2016. Fermentative biohydrogen and biomethane co-production from mixture of food waste and sewage sludge: Effects of physiochemical properties and mix ratios on fermentation performance. Appl. Energy 184, 1–8. doi:10.1016/J.APENERGY.2016.10.003

De Gioannis, G., Friargiu, M., Massi, E., Muntoni, A., Polettini, A., Pomi, R., Spiga, D., 2014. Biohydrogen production from dark fermentation of cheese whey: Influence of pH. Int. J. Hydrogen Energy 39. doi:10.1016/j.ijhydene.2014.10.046

De Gioannis, G., Muntoni, A., Polettini, A., Pomi, R., 2013. A review of dark fermentative hydrogen production from biodegradable municipal waste fractions. Waste Manag. 33, 1345–1361.

De Gioannis, G., Muntoni, A., Polettini, A., Pomi, R., 2009. Electrochemical Remediation Technologies for Polluted Soils, Sediments and Groundwater, Electrochemical Remediation Technologies for Polluted Soils, Sediments and Groundwater. John Wiley & Sons, Inc., Hoboken, NJ, USA. doi:10.1002/9780470523650

De Gioannis, G., Muntoni, A., Polettini, A., Pomi, R., Spiga, D., 2017. Energy recovery from one- and two-stage anaerobic digestion of food waste. Waste Manag. doi:10.1016/j.wasman.2017.06.013

Dong, L., Zhenhong, Y., Yongming, S., Xiaoying, K., Yu, Z., 2009. Hydrogen production characteristics of the organic fraction of municipal solid wastes by anaerobic mixed culture fermentation. Int. J. Hydrogen Energy 34, 812–820. doi:10.1016/j.ijhydene.2008.11.031

Fan, Y., Li, C., Lay, J.-J., Hou, H., Zhang, G., 2004. Optimization of initial substrate and pH levels for germination of sporing hydrogen-producing anaerobes in cow dung compost.

Bioresour. Technol. 91, 189–193. doi:10.1016/S0960-8524(03)00175-5

Ghimire, A., Frunzo, L., Pirozzi, F., Trably, E., Escudie, R., Lens, P.N.L., Esposito, G., 2015. A review on dark fermentative biohydrogen production from organic biomass: Process parameters and use of by-products. Appl. Energy 144, 73–95. doi:10.1016/j.apenergy.2015.01.045

Ghimire, A., Sposito, F., Frunzo, L., Trably, E., Escudié, R., Pirozzi, F., Lens, P.N.L., Esposito, G., 2016. Effects of operational parameters on dark fermentative hydrogen production from biodegradable complex waste biomass. Waste Manag. 50, 55–64. doi:10.1016/j.wasman.2016.01.044

Ghimire, A., Trably, E., Frunzo, L., Pirozzi, F., Lens, P.N.L., Esposito, G., Cazier, E.A., Escudié, R., 2018. Effect of total solids content on biohydrogen production and lactic acid accumulation during dark fermentation of organic waste biomass. Bioresour. Technol. 248, 180–186. doi:10.1016/J.BIORTECH.2017.07.062

Guo, X.M., Trably, E., Latrille, E., Carrere, H., Steyer, J.-P., 2014. Predictive and explicative models of fermentative hydrogen production from solid organic waste: Role of butyrate and lactate pathways. Int. J. Hydrogen Energy 39, 7476–7485. doi:10.1016/j.ijhydene.2013.08.079

Han, W., Ye, M., Zhu, A.J., Huang, J.G., Zhao, H.T., Li, Y.F., 2016. A combined bioprocess based on solid-state fermentation for dark fermentative hydrogen production from food waste. J. Clean. Prod. 112, 3744–3749. doi:10.1016/J.JCLEPRO.2015.08.072

Kim, D.-H., Kim, S.-H., Jung, K.-W., Kim, M.-S., Shin, H.-S., 2011a. Effect of initial pH independent of operational pH on hydrogen fermentation of food waste. Bioresour. Technol. 102, 8646–52. doi:10.1016/j.biortech.2011.03.030

Kim, D.-H., Kim, S.-H., Kim, H.-W., Kim, M.-S., Shin, H.-S., 2011b. Sewage sludge addition to food waste synergistically enhances hydrogen fermentation performance. Bioresour.

Technol. 102, 8501–6.

Kim, S.-H., Han, S.-K., Shin, H.-S., 2006. Effect of substrate concentration on hydrogen production and 16S rDNA-based analysis of the microbial community in a continuous fermenter. Process Biochem. 41, 199–207. doi:10.1016/J.PROCBIO.2005.06.013

Kim, S.H., Han, S.K., Shin, H.S., 2004. Feasibility of biohydrogen production by anaerobic co-digestion of food waste and sewage sludge. Int. J. Hydrogen Energy 29, 1607–1616.

Kobayashi, T., Xu, K.-Q., Li, Y.-Y., Inamori, Y., 2012. Evaluation of hydrogen and methane production from municipal solid wastes with different compositions of fat, protein, cellulosic materials and the other carbohydrates. Int. J. Hydrogen Energy 37, 15711–15718. doi:10.1016/J.IJHYDENE.2012.05.044

Lee, Y.-W., Chung, J., 2010. Bioproduction of hydrogen from food waste by pilot-scale combined hydrogen/methane fermentation. Int. J. Hydrogen Energy 35, 11746–11755. doi:10.1016/j.ijhydene.2010.08.093

Lenth, R.V., 2009. Response-surface methods in R, using rsm. J. Stat. Softw. 32, 1–17.

Liu, D., Liu, D., Zeng, R.J., Angelidaki, I., 2006. Hydrogen and methane production from household solid waste in the two-stage fermentation process. Water Res. 40, 2230–2236. doi:10.1016/J.WATRES.2006.03.029

Liu, Y., 1996. Bioenergetic interpretation on the S0/X0 ratio in substrate-sufficient batch culture. Water Res. 30, 2766–2770. doi:10.1016/S0043-1354(96)00157-1

Ljungdahl, L.G., Hugenholtz, J., Wiegel, J., 1989. Acetogenic and Acid-Producing Clostridia, in: Clostridia. Springer US, Boston, MA, pp. 145–191. doi:10.1007/978-1-4757-9718-3_5

Massanet-Nicolau, J., Dinsdale, R., Guwy, A., Shipley, G., 2013. Use of real time gas production data for more accurate comparison of continuous single-stage and two-stage fermentation. Bioresour. Technol. 129, 561–567. doi:10.1016/J.BIORTECH.2012.11.102

Michel-Savin, D., Marchal, R., Vandecasteele, J.P., 1990. Control of the selectivity of butyric

24

acid production and improvement of fermentation performance with Clostridium tyrobutyricum. Appl. Microbiol. Biotechnol. 32, 387–392. doi:10.1007/BF00903770

Nazlina, H.M.Y., Rahman, N.A., Hasfalina, C.M., Yusoff, M.Z.M., Hassan, M.A., 2011. Microbial characterization of hydrogen-producing bacteria in fermented food waste at different pH values. Int. J. Hydrogen Energy 36, 9571–9580. doi:10.1016/j.ijhydene.2011.05.048

Noblecourt, A., Christophe, G., Larroche, C., Fontanille, P., 2018. Hydrogen production by dark fermentation from pre-fermented depackaging food wastes. Bioresour. Technol. 247, 864–870. doi:10.1016/J.BIORTECH.2017.09.199

Pan, J., Zhang, R., El-Mashad, H.M., Sun, H., Ying, Y., 2008. Effect of food to microorganism ratio on biohydrogen production from food waste via anaerobic fermentation. Int. J. Hydrogen Energy 33, 6968–6975. doi:10.1016/J.IJHYDENE.2008.07.130

R Development Core Team, 2009. R: A language and environment for statistical computing. R Foundation for Statistical Computing, Vienna, Austria.

Reddy, M.V., Hayashi, S., Choi, D., Cho, H., Chang, Y.-C., 2018. Short chain and medium chain fatty acids production using food waste under non-augmented and bio-augmented conditions. J. Clean. Prod. 176, 645–653. doi:10.1016/J.JCLEPRO.2017.12.166

Rodríguez, J., Kleerebezem, R., Lema, J.M., van Loosdrecht, M.C.M., 2006. Modeling product formation in anaerobic mixed culture fermentations. Biotechnol. Bioeng. 93, 592–606. doi:10.1002/bit.20765

Rosales-Colunga, L.M., Razo-Flores, E., De León Rodríguez, A., 2012. Fermentation of lactose and its constituent sugars by Escherichia coli WDHL: Impact on hydrogen production. Bioresour. Technol. 111, 180–184. doi:10.1016/J.BIORTECH.2012.01.175

Saady, N.M.C., 2013. Homoacetogenesis during hydrogen production by mixed cultures dark fermentation: Unresolved challenge. Int. J. Hydrogen Energy 38, 13172–13191.

doi:10.1016/j.ijhydene.2013.07.122

Santos, R.M., Ling, D., Sarvaramini, A., Guo, M., Elsen, J., Larachi, F., Beaudoin, G., Blanpain, B., Van Gerven, T., 2012. Stabilization of basic oxygen furnace slag by hot-stage carbonation treatment. Chem. Eng. J. 203, 239–250.

Schievano, A., Tenca, A., Lonati, S., Manzini, E., Adani, F., 2014. Can two-stage instead of one-stage anaerobic digestion really increase energy recovery from biomass? Appl. Energy 124, 335–342. doi:10.1016/J.APENERGY.2014.03.024

Tawfik, A., El-Qelish, M., 2014. Key factors affecting on bio-hydrogen production from co-digestion of organic fraction of municipal solid waste and kitchen wastewater. Bioresour. Technol. 168, 106–111. doi:10.1016/J.BIORTECH.2014.02.127

Tawfik, A., El-Qelish, M., 2012. Continuous hydrogen production from co-digestion of municipal food waste and kitchen wastewater in mesophilic anaerobic baffled reactor. Bioresour. Technol. 114, 270–274. doi:10.1016/J.BIORTECH.2012.02.016

Van Ginkel, S., Sung, S., Lay, J.-J., 2001. Biohydrogen Production as a Function of pH and Substrate Concentration. Environ. Sci. Technol. 35, 4276–4730. doi:10.1021/ES001979R

Wang, X., Zhao, Y., 2009. A bench scale study of fermentative hydrogen and methane production from food waste in integrated two-stage process. Int. J. Hydrogen Energy 34, 245–254. doi:10.1016/J.IJHYDENE.2008.09.100

Wei, T., Simko, V., 2016. Corrplot: Visualization of a Correlation Matrix.

Zhu, H., Parker, W., Basnar, R., Proracki, A., Falletta, P., Béland, M., Seto, P., 2008. Biohydrogen production by anaerobic co-digestion of municipal food waste and sewage sludges. Int. J. Hydrogen Energy 33, 3651–3659. doi:10.1016/J.IJHYDENE.2008.04.040

Figure captions

Figure 1. Cumulative H_2 production as a function of pH and mixture composition (a, b, c); Plot of t_{95}-H_2 as a function of pH and ISR (d)

Figure 2. Correlation matrix showing the Spearman's rank correlation coefficients for each pair of variables. Blank cells indicate non-significant correlations ($p > 0.05$). The size and colour shade of circles represent the value of the correlation coefficients between pairs of variables (blue shades: positive correlation; red shades: negative correlation)

Figure 3. a) Response surfaces for SHPY (L H_2/kg TOC_{FW}) and b) t_{95}-H_2 (h) as derived from the quadratic model (2)

Figure 4. Time evolution of soluble carbohydrates and TOC as a function of pH and mixture composition

Figure 5. Time evolution of VFAs and ethanol (left-hand y-axis) as a function of pH and mixture composition, and comparison with H_2 production (right-hand y-axis)

Figure 6. a) SHPYobs/SHPYtheor and (Σ metabolic products)/DOC; b) Carbon mass balance for the experimental runs

Table 1. Average composition of FW and AS

Parameter	Unit of measure	FW	AS
pH	-	3.81 ± 0.01	7.08 ± 0.01
Total Solids (TS)	g/L	43.6 ± 2.8	19.3 ± 0.1
Volatile Solids (VS)	g/L	40.2 ± 1.9	14.9 ± 0.4
Total Organic Carbon (TOC)	g/L	25.7 ± 3.9	9.35 ± 1.95
Soluble organic carbon (DOC)	g/L	9.6 ± 0.8	0.55 ± 0.05
Total ammonia	mg N-NH$_4$/L	210.2 ± 8.8	710.2 ± 2.2
Soluble ammonia	mg N-NH$_4$/L	203.9 ± 33.0	615.2 ± 26.4
Total carbohydrates	g hexose/L	13.9 ± 1.9	2.3 ± 0.4
Soluble carbohydrates	g hexose/L	23.1 ± 0.7	0.04 ± 0.003

Table 2. Experimental conditions adopted during the fermentation experiments

Run no.	Run code	Mixture composition (% wet wt.)	ISR (g VS_{AS}/g TOC_{FW})	Operating pH
1	25FW pH5.5	25% FW, 75% AS	1.74	5.5
2	25FW pH6.5	25% FW, 75% AS	1.74	6.5
3	25FW pH7.5	25% FW, 75% AS	1.74	7.5
4	50FW pH5.5	50% FW, 50% AS	0.58	5.5
5	50FW pH6.5	50% FW, 50% AS	0.58	6.5
6	50FW pH7.5	50% FW, 50% AS	0.58	7.5
7	75FW pH5.5	75% FW, 25% AS	0.19	5.5
8	75FW pH6.5	75% FW, 25% AS	0.19	6.5
9	75FW pH7.5	75% FW, 25% AS	0.19	7.5

Table 3. Kinetic parameters of the two-stage Gompertz model and related statistics

		$HPY_{max,1}$ (Nl/kg TOC_{FW})	R_{m1} (Nl/kg $TOC_{FW} \cdot h$)	λ_1 (h)	$HPY_{max,2}$ (Nl/kg TOC_{FW})	R_{m2} (Nl/kg $TOC_{FW} \cdot h$)	λ_2 (h)
		25FW pH 5.5					
	Value	72.44	37.34	3.53	87.82	4.31	0.53
	Std error	0.82	0.71	0.02	0.66	0.08	0.08
$R^2 = 0.9995$	t-value	88.43	52.51	149.85	133.91	53.23	6.62
Fit std. error = 1.0485	95% conf.	70.83	35.93	3.48	86.53	4.15	0.37
	limits	74.06	38.74	3.57	89.12	4.47	0.69
		50FW pH 5.5					
	Value	114.22	29.40	3.55	42.20	8.99	13.39
	Std error	0.51	0.51	0.03	0.61	0.36	0.12
$R^2 = 0.9986$	t-value	223.04	57.60	104.01	69.71	25.31	109.83
Fit std. error = 2.0153	95% conf.	113.21	28.39	3.48	41.01	8.29	13.15
	limits	115.23	30.41	3.62	43.40	9.69	13.63
		75FW pH 5.5					
	Value	72.85	5.57	31.47	3.65	0.11	78.53
	Std Error	0.10	0.04	0.05	0.36	0.01	2.17
$R^2 = 0.9990$	t-value	753.63	142.78	653.34	10.05	8.09	36.17
Fit std. error = 1.0125	95% conf.	72.66	5.49	31.37	2.94	0.08	74.27
	limits	73.04	5.64	31.56	4.37	0.14	82.79
		25FW pH 6.5					
	Value	58.06	3.46	0.67	70.41	59.38	3.18
	Std Error	0.81	0.09	0.08	0.67	1.09	0.01
$R^2 = 0.9997$	t-value	71.62	38.84	8.70	105.33	54.51	236.49
Fit std. error = 0.7725	95% conf.	56.45	3.29	0.52	69.09	57.22	3.15
	limits	59.67	3.64	0.82	71.74	61.54	3.21
		50FW pH 6.5					
	Value	99.05	47.92	3.26	25.52	5.12	7.23
	Std Error	0.73	0.77	0.02	0.76	0.17	0.18
$R^2 = 0.9994$	t-value	135.21	62.46	211.03	33.38	30.66	40.25
Fit std. error = 1.0357	95% conf.	97.60	46.40	3.23	24.01	4.79	6.88
	limits	100.50	49.43	3.29	27.03	5.45	7.59
		75FW pH 6.5					
	Value	56.85	31.70	4.55	59.61	4.20	2.88
	Std Error	0.73	0.57	0.02	0.64	0.09	0.07
$R^2 = 0.9997$	t-value	78.10	55.23	211.82	93.43	47.68	41.08
Fit std. error = 0.7467	95% conf.	55.41	30.57	4.50	58.35	4.02	2.74
	limits	58.28	32.84	4.59	60.87	4.37	3.02
		25FW pH 7.5					
	Value	40.34	32.39	2.35	1.14	0.83	10.33
	Std Error	0.10	0.72	0.01	0.10	0.60	0.57
$R^2 = 0.9926$	t-value	404.18	45.15	156.83	11.00	1.37	17.97
Fit std. error = 0.5782	95% conf.	40.14	30.98	2.32	0.93	-0.36	9.20
	limits	40.53	33.80	2.38	1.34	2.01	11.46
		50FW pH 7.5					
	Value	76.36	30.31	2.63	1.08	3630.00	-90.88
	Std Error	0.32	2.27	0.05	0.33	1.91	1.82
$R^2 = 0.9951$	t-value	241.35	13.33	55.40	3.31	1900.96	-49.87
Fit std. error = 1.8329	95% conf.	75.73	25.81	2.54	0.44	3626.23	-94.48
	limits	76.99	34.81	2.73	1.73	3633.77	-87.28
		75FW pH 7.5					
	Value	82.20	31.35	4.26	15.63	2.46	11.67
	Std Error	0.28	0.44	0.02	0.34	0.11	0.21
$R^2 = 0.9992$	t-value	291.67	70.85	225.49	45.79	21.44	54.32
Fit std. error = 0.9831	95% conf.	81.65	30.48	4.23	14.96	2.24	11.25
	limits	82.76	32.23	4.30	16.31	2.69	12.10
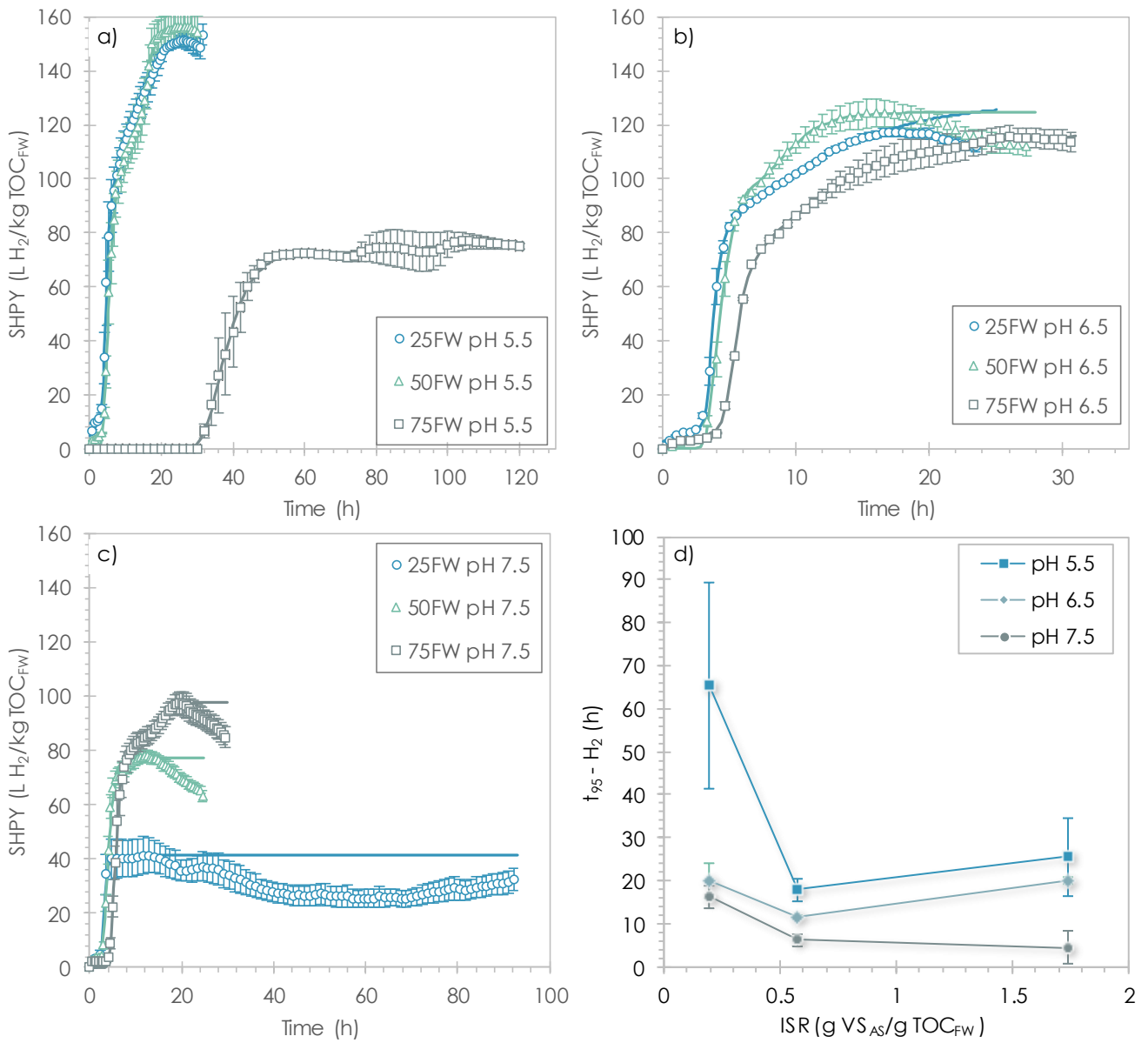
Figure 1

Figure 2

SHPY (L H2/kg TOC(FW))

t95-H2 (h)
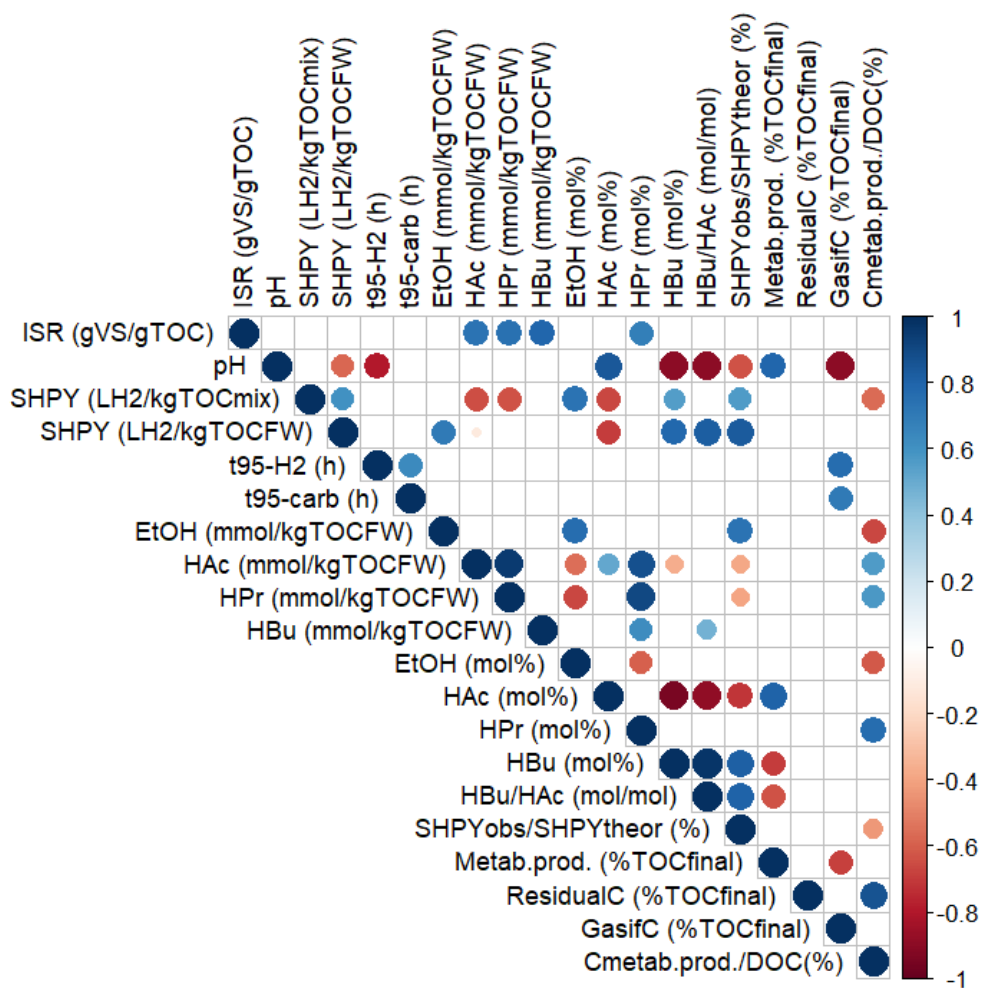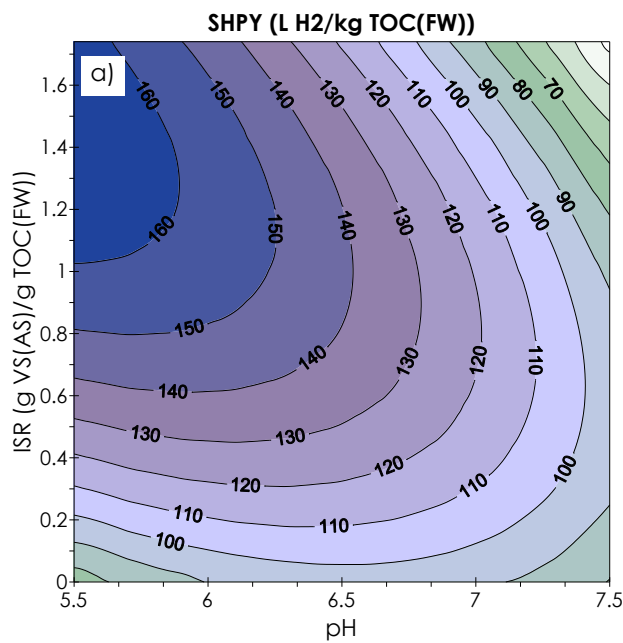
Results of the ANOVA for SHPY
Multiple R^2 = 0.8063

	Df	Sum Sq	Mean Sq	F value	Pr(>F)
Linear (pH, ISR)	2	10257.5	5128.8	12.44	0.0012
Quadratic (pH, ISR)	2	2806.5	1403.3	3.40	0.0674
Interaction (pH, ISR)	1	7519.3	7519.3	18.24	0.0011
Residuals	12	4945.7	412.1		
Lack of fit	3	3102.2	1034.1	5.05	0.0254
Pure error	9	1843.5	204.8		
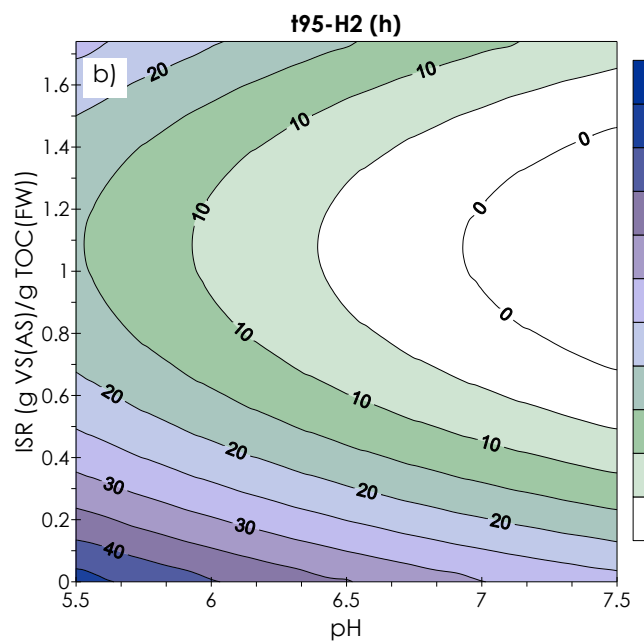
Results of the ANOVA for t95-H2
Multiple R^2 = 0.8769

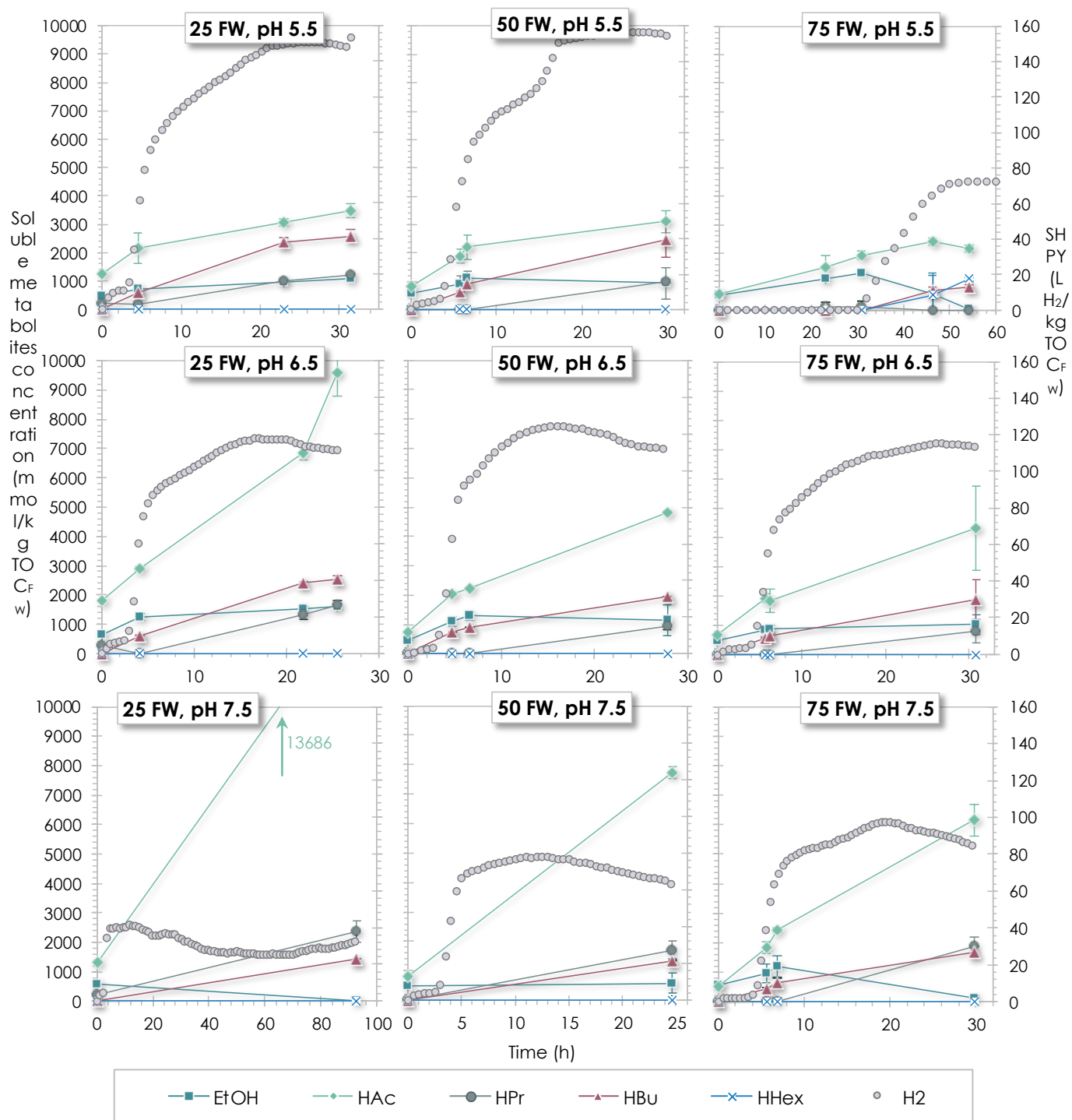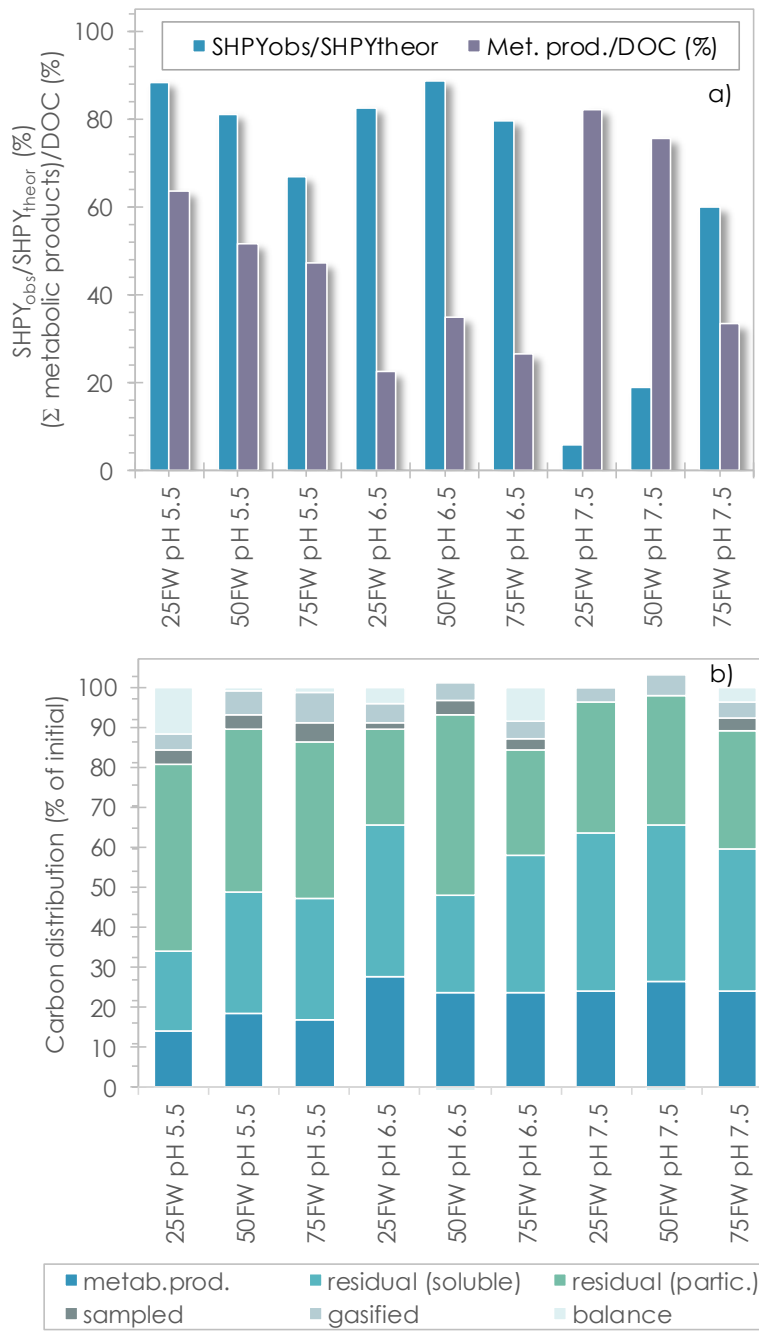|	Df	Sum Sq	Mean Sq	F value	Pr(>F)
Linear (pH, ISR)	2	640.08	320.04	7.46	0.0685
Quadratic (pH, ISR)	2	276.43	138.22	3.2218	0.1791
Interaction (pH, ISR)	1	0.45	0.45	0.0104	0.9252
Residuals	3	128.7	42.9		
Lack of fit	3	128.7	42.9		
Pure error	0	0			

Figure 3
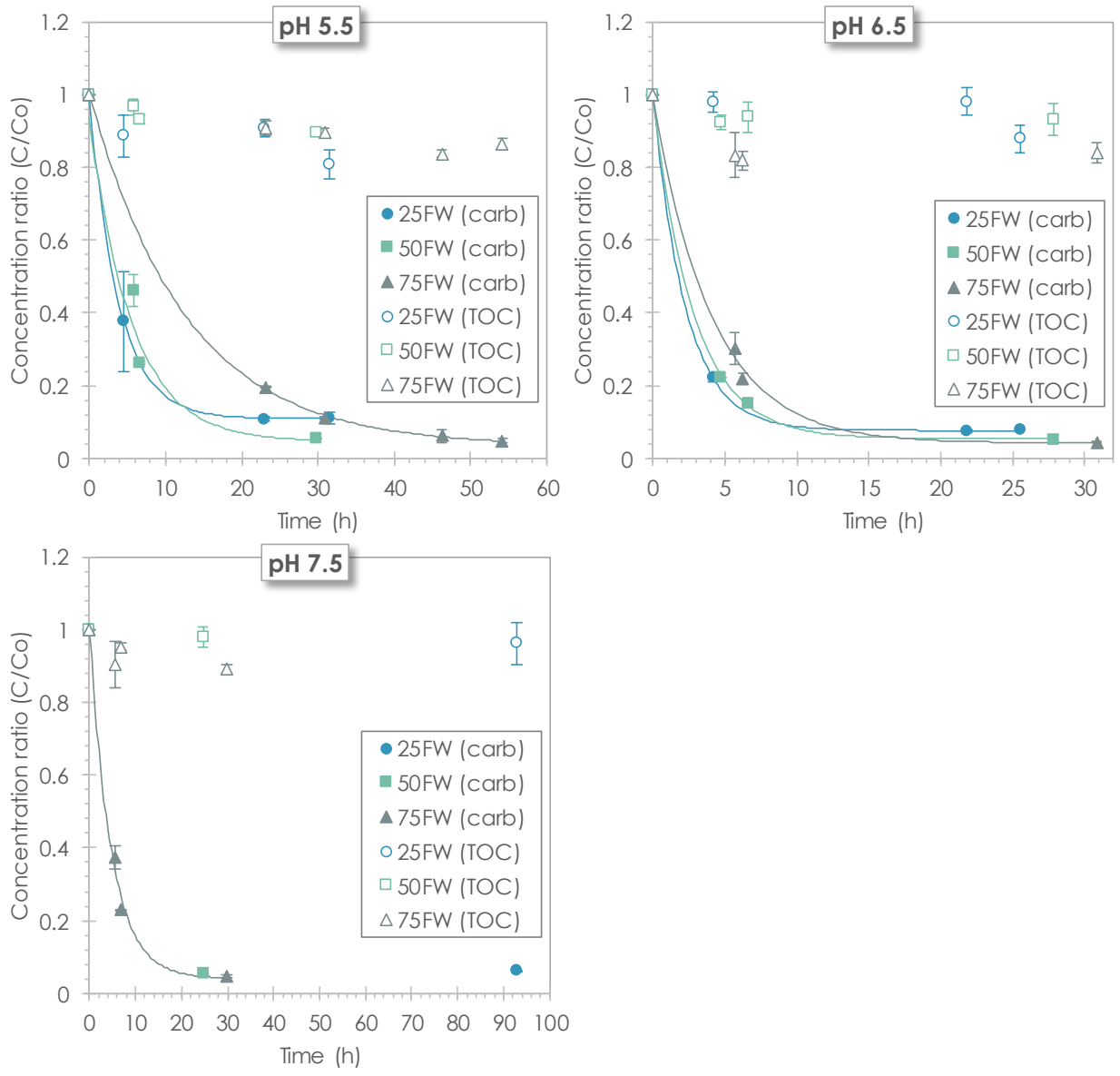
3

Figure 4

Figure 5

Figure 6

Electronic Annex

Click here to download Electronic Annex: Supplementary Information.docx